Thermochimica Acta, 33 (1979) 127—140

THERMOGRAVIMETRIC STUDY ON THE DECOMPOSITION OF HYDROMAGNESITE 4 $MgCO_3 \cdot Mg(OH)_2 \cdot 4\ H_2O$

YUTAKA SAWADA, JUNJI YAMAGUCHI, OSAMU SAKURAI, KEIZO UEMATSU, NOBUYASU MIZUTANI and MASANORI KATO

Department of Inorganic Materials, Faculty of Engineering, Tokyo Institute of Technology, O-okayama, Meguro-ku, Tokyo 152 (Japan)

(Received 14 November 1978)

ABSTRACT

Isothermal and non-isothermal decomposition of hydromagnesite 4 $MgCO_3 \cdot Mg(OH)_2 \cdot 4\ H_2O$ was studied thermogravimetrically. Decarbonation was strongly influenced by the partial pressure of carbon dioxide. Decarbonation in an argon atmosphere proceeded via an amorphous lower carbonate to MgO. Decarbonation in a carbon dioxide atmosphere was interrupted at ~460—480°C. This interruption was explained by the formation of a metastable intermediate and the subsequent crystallization of $MgCO_3$, both from the amorphous lower carbonate. This explanation was supported by DTA and powder X-ray diffraction analysis of the quenched specimens.

INTRODUCTION

Thermal decomposition of hydromagnesite 4 $MgCO_3 \cdot Mg(OH)_2 \cdot 4\ H_2O$ proceeds via dehydration (<300°C) and decarbonation (>350°C) towards MgO. The decarbonation is highly dependent on the partial pressure of carbon dioxide (P_{CO_2}) [1—7]; decarbonation type I ($P_{CO_2} \leqslant 0.1$ kg cm^{-2}), type II (typical $P_{CO_2} \simeq 1$ kg cm^{-2}) and type III (typical $P_{CO_2} \simeq 10$ kg cm^{-1}) were found when the specimen was heated non-isothermally (heating rate: ~ 10°C min^{-1}) [1—3]. In type I, the decarbonation of the amorphous dehydrated phase proceeded via the amorphous lower carbonate phase to MgO, this decarbonation process being called "stage 1". In type II, stage 1 was interrupted gradually. Crystallization of $MgCO_3$ took place suddenly at ~500°C with a sharp exothermic phenomenon and rapid evolution of a small amount of carbon dioxide (stage 2). The $MgCO_3$ decomposed to MgO at the higher temperature (stage 3). In type III, stage 1 was just evident. The crystalline intermediate reported by Suzuki et al. [8] was formed with increased CO_2/MgO molar ratio of the specimen (stage 1'). The immediate disappearance of the intermediate was accompanied by a decrease in the CO_2/MgO molar ratio and crystallization of $MgCO_3$ (stage 2'). Decarbonation of the $MgCO_3$ proceeded at the higher temperature (stage 3).

The following explanations were given in previous papers [1—3] for the non-isothermal decomposition processes.

(1) The formation of the intermediate prevented the decarbonation stage 1 in a carbon dioxide atmosphere.

(2) The exothermic phenomenon was due to the crystallization of $MgCO_3$ from the amorphous lower carbonate.

(3) The rapid evolution of carbon dioxide was due to decarbonation caused by the heat of $MgCO_3$ crystallization.

These explanations were successfully confirmed in the present study by thermogravimetry. The decarbonation mechanisms were investigated on (1) the dehydrated specimen (the amorphous lower carbonate) and (2) the $MgCO_3$ specimen quenched immediately after stage 2. Both isothermal and non-isothermal ($\sim 10°C\ min^{-1}$) conditions were adopted in argon and carbon dioxide atmospheres. The isothermal decomposition of the amorphous lower carbonate at 460—510°C was studied in detail by DTA and powder X-ray diffraction analysis since the remarkable formation of the intermediate and crystallization of $MgCO_3$ took place under these conditions.

EXPERIMENTAL

Specimens

Hydromagnesite

Magnesium hydroxide carbonate G.R. (Merck, West Germany) was used. The powder X-ray diffraction diagram was identified as hydromagnesite [9]. No other compound was present. The $MgO : CO_2 : H_2O$ molar ratios were 1.000 : 0.775 : 1.117. The specimen was a fine white powder. Each particle was a platelet of ~0.1—1.0 μm in length and ~0.05 μm in thickness. No control was made over the particle size. Electron diffraction showed that each particle was polycrystalline.

Lower carbonate

The hydromagnesite was dehydrated in order to investigate the decarbonation process intensively: the hydromagnesite was heated in a mixture of helium and carbon dioxide ($P_{CO_2} = 0.50\ kg\ cm^{-2}$) at $\sim 10°C\ min^{-1}$ until 350°C, when only the dehydration was completed, and then quenched. The $MgO : CO_2 : H_2O$ molar ratios were 1.000 : 0.766 : 0.372. Slight decarbonation occurred during this treatment and the lower carbonate was also formed. The apparent water content was due to the absorbed water as will be described later.

$MgCO_3$

The hydromagnesite was heated under the same conditions as above to ~520°C, where the sudden crystallization of $MgCO_3$ and the rapid evolution of carbon dioxide were completed, then quenched. The $MgO : CO_2 : H_2O$ molar ratios were 1.000 : 0.564 : 0.204. The specimen showed the powder X-ray diffraction pattern of $MgCO_3$ [10].

Thermobalance

The outline of the thermobalance is shown in Fig. 1A and B. The balance was a modified chemical balance. The weight change was measured by a

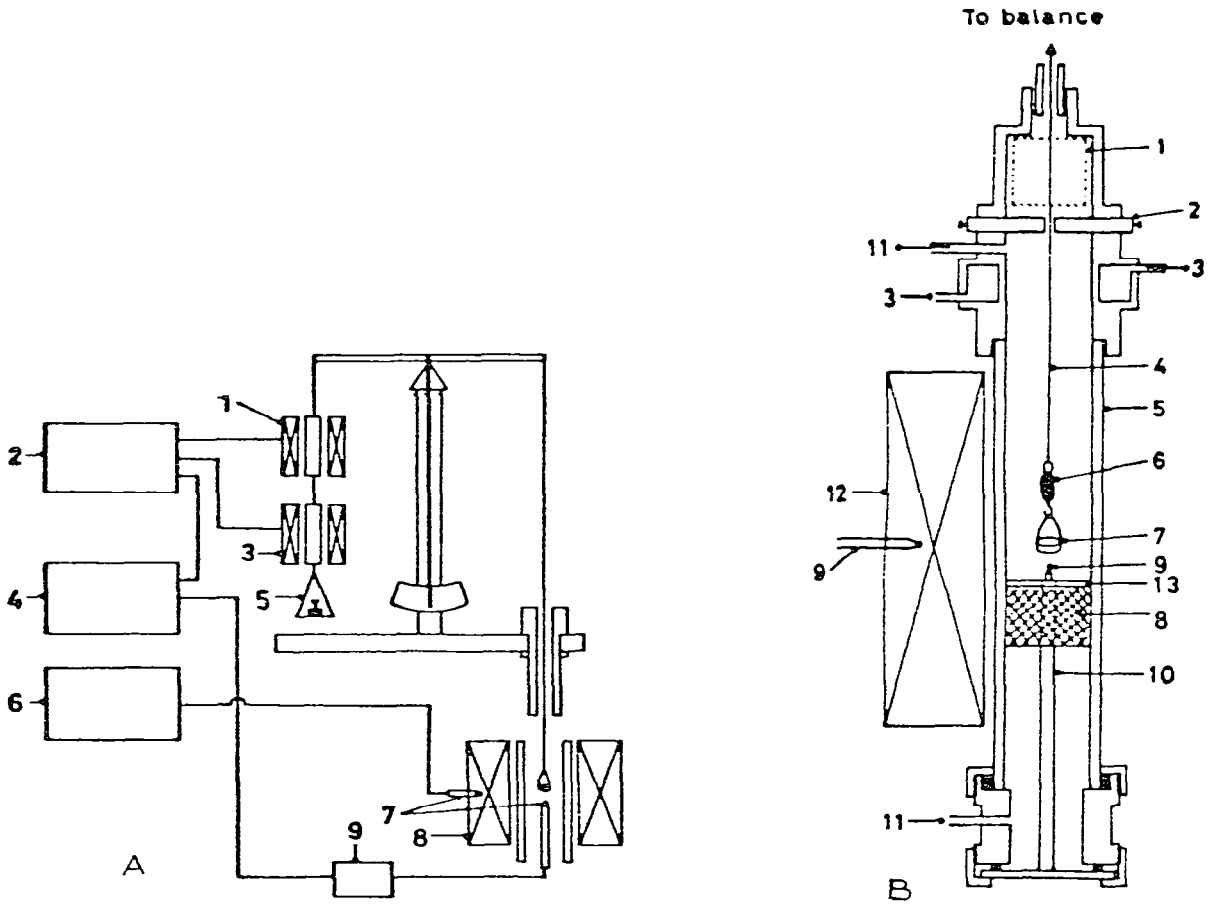

Fig. 1 A, Construction of the thermobalance. 1, Force coil; 2, amplifier; 3, differential transformer; 4, strip chart recorder; 5, balancing weight; 6, temperature controller (Chino Works Ltd., Japan, E505 type); 7, thermocouple (Pt—PtRh 13%) for temperature control; 8, furnace; 9, cold junction (0°C). B, Construction of the thermobalance. 1, Window for sample change; 2, sliding shutters with a hole (5 mm diam.) for the platinum wire (4); 3, cooling water inlet and outlet; 4, platinum wire (0.1 mm diam.); 5, mullite tube; 6, stabilizer: a platinum weight (1.5 g); 7, specimen holder (platinum, 15 mm diam., 0.3 g); 8, buffer (porous fire block); 9, thermocouple for temperature measurement (Pt—Pt/13% Rh); 10, alumina tube; 11, gas inlet and outlet (argon or carbon dioxide); 12, furnace (Kantal double-wound induction-free furnace); 13, alumina plate (the gas passed through the gap between the plate and the furnace tube).

detection unit (Shinko Denki Co., Ltd., Japan) based on a differential transformer and was recorded on a strip-chart recorder. At maximum, a specimen of 100 g could be placed on the balance. The maximum weight range was either 5 or 50 mg and the sensitivity was 0.02 mg. The maximum temperature was 700°C. The rate of temperature change was 0—20°C min^{-1} in both directions. A blank test was made before each run; the TG curve was calibrated by the blank test. The specimen holder containing the specimen (~7 mg) was inserted into the predetermined position quickly for the isothermal experiments; a direct measurement with a thin thermocouple showed that the temperature of the specimen reached the predetermined temperature within a minute. The gas flow (argon or carbon dioxide, linear

flow velocity ~5 cm min^{-1}) was provided. The specimen was heated at ~8—10°C min^{-1} in the case of the non-isothermal experiments.

To account for the water content in the specimen, it was assumed that the water was removed first and carbon dioxide was removed later at the higher temperature. Weight loss data were converted into fractional decomposition (α) versus time for further evaluation; $\alpha = 0$ was defined for the CO_2/MgO molar ratio as 0.975 for the hydromagnesite specimen, 0.766 for the lower carbonate specimen and 0.564 for the $MgCO_3$ specimen, respectively.

Estimation of termination temperature

The non-isothermal decarbonation processes under various conditions were compared: temperatures where the non-isothermal decompositions apparently terminated were estimated from the data of isothermal experiments. The temperatures at which the isothermal decomposition rates were 3×10^{-3} (sec^{-1}) in Fig. 5 were assumed to be the termination temperatures; the interpolation was adopted for the $MgCO_3$ and the extrapolation was adopted for the lower carbonate.

The value of 3×10^{-3} (sec^{-1}) was chosen for the following reason: when the specimens were heated at ~10°C min^{-1} in DTA, TG or DTGA [1,2], the half-widths were approximately 50—100°C which correspond to 300—600 sec. Assuming that the non-isothermal decompositions were mostly completed in 300—600 sec, the average decomposition rate ($d\alpha/dt$) was approximately 1.5×10^{-3}—3×10^{-3} (sec^{-1}). The decomposition was near completion when the rate was 3×10^{-3} (sec^{-1}) in the non-isothermal experiment.

DTA—TG

DTA and TG was studied with a DTA—TG type M8076, Rigaku Denki Co., Japan in a carbon dioxide atmosphere with specimen weight of ~16 mg. The specimen was heated at the rate of ~10°C min^{-1} to a predetermined temperature (~460—510°C) where the decarbonation rate was very slow. After being held at that temperature for a predetermined period (up to 2 h), the specimen was quenched to room temperature for powder X-ray diffraction analysis.

Powder X-ray diffraction analysis

The powder X-ray diffractions were recorded; Philips APD-10, target: Cu 45kV 30 mA, graphite monochromator, automatic divergence slit, scan speed: $2\theta = 4$°C min^{-1}. The phases were identified automatically by the computer incorporating a search—match program.

RESULTS

Non-isothermal method

Non-isothermal thermogravimetric records for the decomposition of hydromagnesite are shown in Fig. 2. Decarbonation occurred at 300—600°C. It was markedly influenced by the partial pressure of carbon dioxide. The decarbonation stages 1, 2 and 3 were observed in a carbon dioxide atmo-

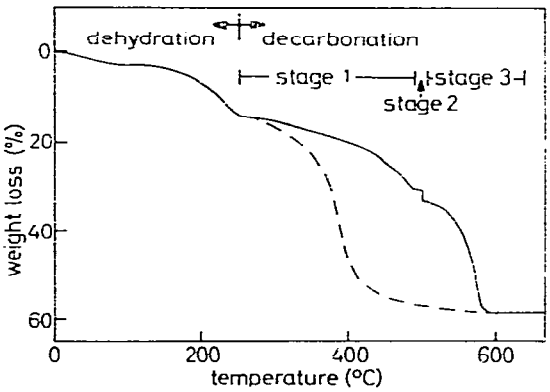

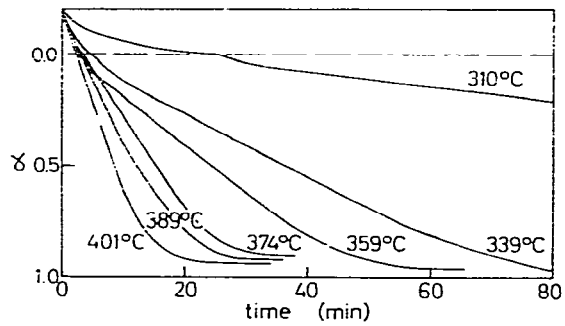

Fig. 2. Thermal decomposition of hydromagnesite by non-isothermal thermogravimetry. ———, Carbon dioxide atmosphere; - - - - - -, argon atmosphere; specimen weight, 7 mg; heating rate, 8—10°C min^{-1}. Dehydration was observed below 300°C in both atmospheres. Only the decarbonation stage 1 was found in an argon atmosphere. The decarbonation stages 1, 2 and 3 were found in a carbon dioxide atmosphere.

Fig. 3. The relation between the fraction decomposed (α) and the heating time. Isothermal method, specimen: the lower carbonate (~7 mg); atmosphere: argon. The negative value in the fraction decomposed (α) was due to the residual water in the specimen.

sphere (type II). Only the decarbonation stage 1 was observed in an argon atmosphere (type I). Dehydration was found below 300°C. It was not affected by the partial pressure of carbon dioxide.

Lower carbonate

Argon atmosphere

The fraction of specimen decomposed (α) at a constant temperature in an argon atmosphere are plotted against the heating time in Fig. 3. The discontinuity at $\alpha = 0$ at 310°C showed that the dehydration took place prior to the decarbonation. Results at the higher temperatures did not show such a discontinuity. The dehydration was probably completed before the temperature of the specimen reached the predetermined point. The decomposition above 339°C showed a linear relation for $\alpha = 0.3$—0.7. Approximately zero-order kinetics were applicable for the decomposition process. The decarbonation rates ($d\alpha/dt$) at $\alpha = 0.5$ are presented for various temperatures in Fig. 4. The decarbonation rates ($d\alpha/dt$) calculated using the results of the non-isothermal method ($\alpha \neq 0.5$) are also included in this figure. The decrease in the decarbonation rate was found at ~400°C in the non-isothermal method. This was due to the completion of the decarbonation. Approximately the same decarbonation rates were obtained by isothermal and non-isothermal methods. The Arrhenius plots of these decarbonation rates are shown in Fig. 5. The activation enthalpy was found to be 27.5 kcal $mole^{-1}$.

Carbon dioxide atmosphere

The fraction decomposed (α) is plotted against the heating time in Figs. 6A, B and C for the isothermal decomposition of the lower carbonate speci-

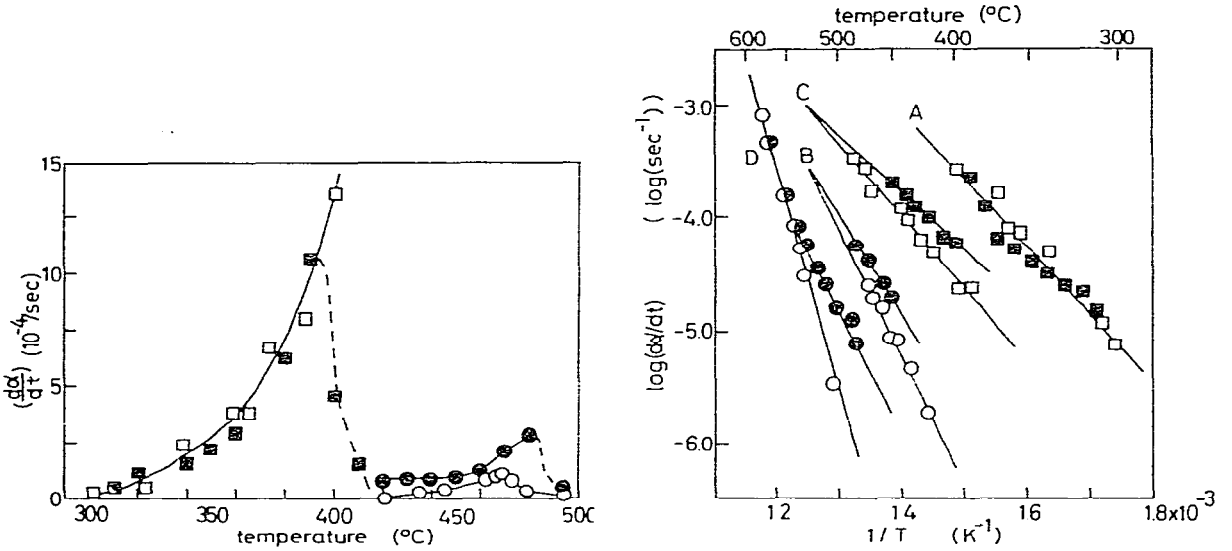

Fig. 4. Decarbonation rates ($d\alpha/dt$) of the lower carbonate at various temperatures. □, ■, Argon atmosphere; ○, ●, carbon dioxide atmosphere. □, ○, Isothermal method (the lower carbonate was used. The decarbonation rates at $\alpha = 0.5$ at various temperatures are plotted); ■, ●, non-isothermal method (hydromagnesite was used. The decarbonation rates at various temperatures are plotted; α is not necessarily 0.5).

Fig. 5. Arrhenius plots of the decarbonation rate ($d\alpha/dt$). The lower carbonate. A, argon atmosphere: □, isothermal method; ■, non-isothermal method. B, carbon dioxide atmosphere: ○, isothermal method; ●, non-isothermal method. $MgCO_3$. C, argon atmosphere: □, isothermal method; ■, non-isothermal method. D, carbon dioxide atmosphere: ○, isothermal method; ●, non-isothermal method. Hydromagnesite was used in the non-isothermal method (A, B, C and D). The lower carbonate specimen obtained by quenching the hydromagnesite immediately after the dehydration was used in the isothermal method (A and B). The $MgCO_3$ specimen obtained by quenching the hydromagnesite immediately after the exothermic phenomenon (stage 2 of type II) was used in the isothermal method (C and D).

men in a carbon dioxide atmosphere. The decomposition rate increased as the temperature increased at 421—469°C (Fig. 6A). Sigmoidal curves were observed below 451°C. These curves were approximately linear for $\alpha = 0.4$—0.6.

The decarbonation rates ($d\alpha/dt$) at $\alpha = 0.5$ are shown in Fig. 4 for various temperatures. The decarbonation rates calculated from the results of the non-isothermal method are also shown in this figure. The decarbonation rates were greater under non-isothermal conditions than under isothermal conditions; the relative deviation was much greater in a carbon dioxide atmosphere than in an argon atmosphere. Figure 5 shows the Arrhenius plots of these decarbonation rates in a carbon dioxide atmosphere. The activation enthalpy of the process was 56.5 kcal mole^{-1} in the isothermal method and 35.1 kcal mole^{-1} in the non-isothermal method.

At high temperatures (469—487°C) as shown in Fig. 6B, the decarbonation rate decreased with increasing temperature. The decarbonation was apparently interrupted at ~475°C after ~200 min.

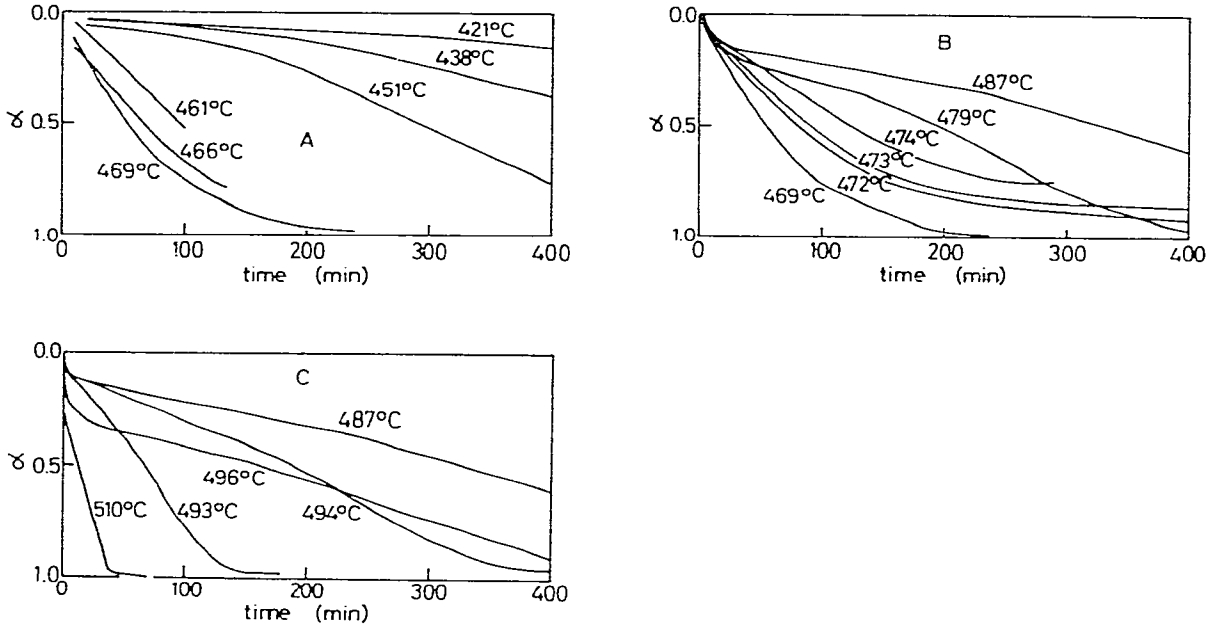

Fig. 6. Fraction decomposed (α) and the heating time. Isothermal method, specimen: the lower carbonate (~7 mg); atmosphere: carbon dioxide. A, The decarbonation rate ($d\alpha/dt$) increased as the temperature increased at 421—469°C. B, The decarbonation rate decreased as the temperature increased at 469—487°C. C, The decarbonation was influenced significantly by the slight differences in the experimental conditions at 487—510°C.

At still higher temperatures (487—500°C), as shown in Fig. 6C, completely different curves were obtained at approximately the same temperatures; typical examples are shown in this figure.

At ~500—510°C, the decarbonation rate increased again with increasing temperature. However, crystallization of $MgCO_3$ took place while the specimen was being inserted into the predetermined position in the thermobalance; the specimen powders were explosively dispersed which made further measurement impossible.

This strange decomposition behavior will be discussed later.

$MgCO_3$

Argon atmosphere

The fractions of $MgCO_3$ decomposed (α) in an argon atmosphere under isothermal conditions are plotted against the heating time in Fig. 7. An approximately linear relation was found for $\alpha = 0.0$—0.7; then the decarbonation rate decreased gradually. The decarbonation rate increased with increasing temperature. The Arrhenius plots of the decarbonation rates at $\alpha = 0.5$ are shown in Fig. 5. The decarbonation rates under non-isothermal conditions are shown in this figure. The isothermal decarbonation rates were smaller than the corresponding non-isothermal decarbonation rates. The activation enthalpy of the decarbonation process was 24.3 kcal mole^{-1} for the isothermal and 29.0 kcal mole^{-1} for the non-isothermal conditions.

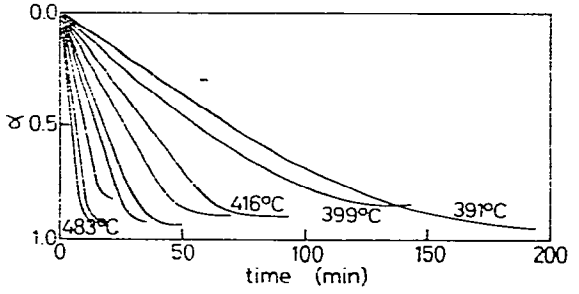

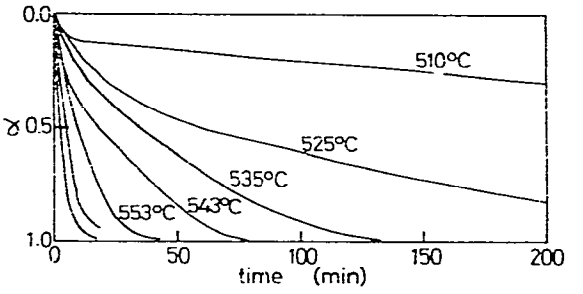

Fig. 7. Fraction decomposed (α) and the heating time. Isothermal method, specimen: $MgCO_3$ (~7 mg); atmosphere: argon.

Fig. 8. Fraction decomposed (α) and the heating time. Isothermal method, specimen: $MgCO_3$ (~7 mg); atmosphere: carbon dioxide.

Carbon dioxide atmosphere

The fraction decomposed (α) against the heating time for the $MgCO_3$ under non-isothermal conditions in a carbon dioxide atmosphere is shown in Fig. 8. The decarbonation rate decreased gradually as the decomposition progressed. The linear approximation was applicable for a relatively short range. No sigmoidal curves appeared.

The Arrhenius plots of these decarbonation rates at $\alpha = 0.5$ are shown in Fig. 5. The activation enthalpy for the process was 81.7 kcal $mole^{-1}$. In this figure, the decarbonation rates obtained from the non-isothermal method are also plotted. The non-isothermal decarbonation rates were larger than the isothermal decarbonation rates below 540°C; the activation enthalpy of the non-isothermal process was 56.4 kcal $mole^{-1}$. The isothermal decarbonation rates were the same as the non-isothermal decarbonation rates above 540°C.

Comparison of the various decarbonations

The decarbonation processes under the various conditions were compared: the non-isothermal termination temperatures estimated from the isothermal data were compared with the experimental non-isothermal termination temperatures. Good agreements were obtained; the estimated and the experimental values were 400 and 400°C for the lower carbonate in an argon atmosphere, 480 and 500°C for the $MgCO_3$ in an argon atmosphere and 560 and 600°C for the $MgCO_3$ in a carbon dioxide atmosphere, respectively. The lower carbonate in a carbon dioxide atmosphere was an exception since the non-isothermal decomposition was not completed. The decarbonation was interrupted below 500°C although the estimated termination temperature was 530°C.

DTA—TG and powder X-ray diffraction analysis

The isothermal decarbonation at ~460—510°C in a carbon dioxide atmosphere (Fig. 6B and C) was investigated with DTA—TG. A typical example is shown in Fig. 9. The temperature program is shown in Fig. 9A; the specimen was heated at ~10°C min^{-1} to 480°C and held at that temperature. The results of TG and DTA are shown in Fig. 9B and C, respectively. The results of powder X-ray diffraction analysis on the specimens quenched after

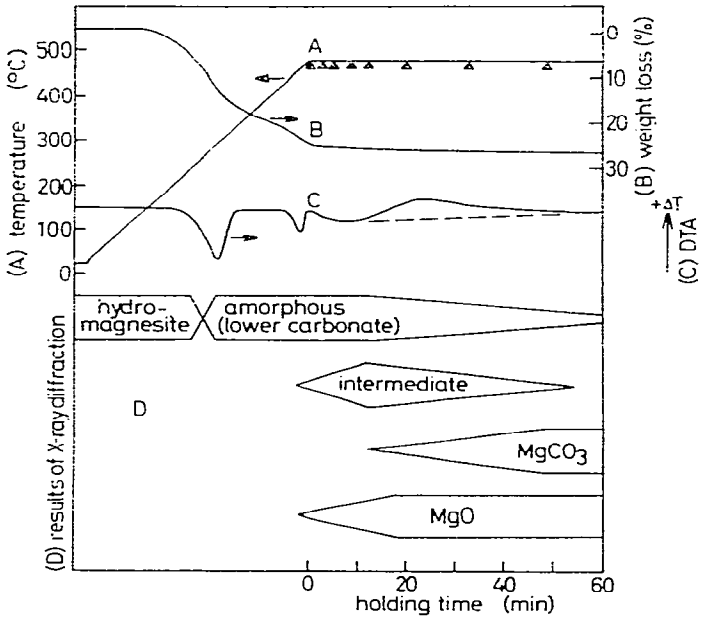

Fig. 9. Results of TG—DTA and powder X-ray diffraction analysis for hydromagnesite. Specimen: hydromagnesite (~16 mg); heating rate: 10°C min^{-1}, holding temperature: 480°C, atmosphere: carbon dioxide. A, Temperature (▲, specimens were quenched for powder X-ray diffraction analysis the results of which are shown in Figs. 9D and 10); B, TG; C, DTA; D, Phases present in the specimen (the width of the band gives a rough idea of the amount in each phase).

various holding times are shown in Fig. 10. The phases present in the specimen and their amount are summarized in Fig. 9C.

The decarbonation proceeded inhomogeneously; the phases present are what the authors call the amorphous lower carbonate, the intermediate [3,8], $MgCO_3$ and MgO. The dominant phase changed as the decarbonation process progressed; the amorphous lower carbonate in the first place, then the intermediate, $MgCO_3$ and finally MgO. The sequential order of the dominant phase was the same in the non-isothermal decarbonation type III which

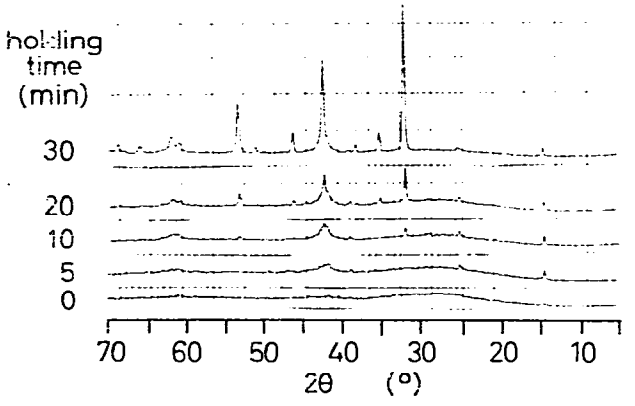

Fig. 10. Powder X-ray diffraction of the hydromagnesite quenched after the various heating periods. Specimens were quenched from the condition shown by ▲ in Fig. 9A.

was observed in high-pressure carbon dioxide atmospheres as that reported in a previous paper [3]. Only MgO was thermodynamically stable in this condition [11].

When the specimen was heated at ~10°C min^{-1}, the dehydration was completed at ~300°C (TG and DTA) where the amorphous phase was observed (powder X-ray diffraction). The maximum of the decarbonation stage 1 occurred at ~465°C (TG and DTA).

The specimen was held at a constant temperature (480°C). Slight decarbonation was observed during the first 10 min where very slight weight loss and a very slight endothermic peak were observed. The X-ray diffraction peaks of the intermediate were observed. Its diffraction peak intensity increased gradually with time; maximum at ~10 min. Neither the strong exothermic peak nor the coincident sudden weight loss was observed. The very broad diffraction peaks of MgO appeared and their diffraction intensities increased gradually as the decarbonation proceeded very slowly; only the strongest two diffraction peaks, (200) and (220) at 2θ = 42.94° and 62.68°, respectively, were observed like haloes.

Very broad exothermic peaks (DTA) were found at ~10—40 min when the diffraction peaks of $MgCO_3$ appeared and their intensities increased gradually. Weight loss was extremely slow being near the detection limit of TG. A shrinkage of the packed specimen powders was observed. The diffraction intensity of the intermediate decreased gradually. The diffraction intensity of MgO was constant; the observation was rather difficult since the diffraction peaks were overlapped by the much stronger $MgCO_3$ diffraction peaks.

Results of DTA for hydromagnesite with various holding temperatures are shown in Fig. 11. The time taken for the exothermic phenomenon to occur decreased as the holding temperature increased. The temperature for the crystallization of $MgCO_3$ was not restricted to ~500°C. The crystallization took place at a lower temperature e.g. 470°C in the case of the isothermal decomposition. The coincident sudden weight loss was observed at ~500—510°C when the specimens were heated continuously without holding.

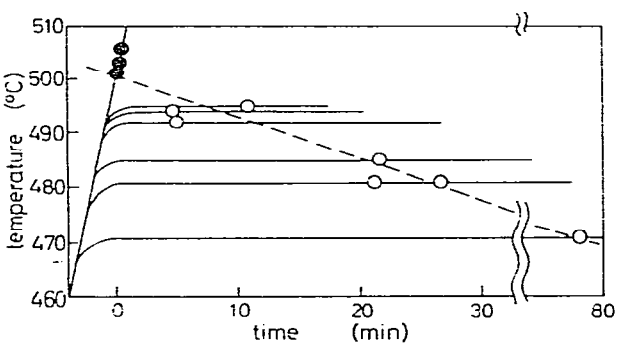

Fig. 11. DTA for hydromagnesite with various holding temperatures. ———, Heating schedule; ●, an exothermic phenomenon with a sudden weight loss; ○, and exothermic phenomenon without a weight loss. Specimen: hydromagnesite (~16 mg); atmosphere: carbon dioxide.

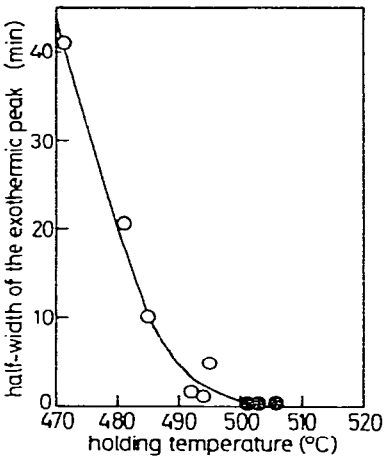

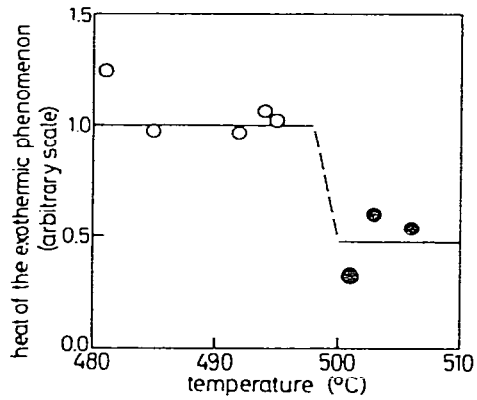

Fig. 12. Change of half-width of the exothermic peak with the holding temperature. ●, An exothermic phenomenon with a sudden weight loss; ○, an exothermic phenomenon without a weight loss. Specimen: hydromagnesite (~16 mg); atmosphere: carbon dioxide.

Fig. 13. The effect of holding temperature on the heat of the exothermic phenomenon. ●, An exothermic phenomenon with a sudden weight loss; ○, an exothermic phenomenon without a weight loss. Specimen: hydromagnesite (~16 mg); atmosphere: carbon dioxide.

Half-widths of the exothermic peak are plotted against the holding temperature or the temperature of the exothermic phenomenon in Fig. 12. The peak became sharper as the holding temperature increased. Peak width and the period required for the exothermic phenomenon to appear represent approximately the rates of the process associated with them. Minus the logarithm of the half-width was plotted against the reciprocal absolute holding temperature (not shown). Minus the logarithm of the period required for the exothermic phenomenon to appear was plotted against the absolute holding temperature (not shown). The activation energies calculated tentatively were ~100—300 kcal mole^{-1} for both cases. The rate determining factor was influenced very strongly by the temperature.

The heat associated with the exothermic phenomenon is plotted against the holding temperature in Fig. 13. The heat was approximately constant except when the specimens were heated without holding.

DISCUSSION

The decarbonation of the lower carbonate proceeded via the metastable intermediate and $MgCO_3$ in a carbon dioxide atmosphere. This process was easier than the direct decomposition to MgO which was thermodynamically stable.

Strange behavior was found in the isothermal decarbonation of the lower carbonate in a carbon dioxide atmosphere at 469—487°C (Fig. 6B); the decomposition rate decreased as the temperature increased. This behavior can be explained by the formation of the intermediate and $MgCO_3$. The lower decomposition rate of the intermediate and $MgCO_3$ relative to the

lower carbonate reduced the apparent decomposition rate. The formation of the metastable intermediate and $MgCO_3$ under these conditions was confirmed by X-ray diffraction analysis (Fig. 10). Interruption of the non-isothermal decarbonation in a carbon dioxide atmosphere at ~500°C (Fig. 2) can also be understood in terms of the formation of the intermediate. The isothermal decomposition in the temperature range of 487—510°C (Fig. 6C) was extremely random. This result strongly suggests that the isothermal decomposition was influenced markedly by the intermediate which was formed during the heating period (approximately 1 min); minute differences in the preheating conditions influenced the formation of the intermediate and the $MgCO_3$, and the subsequent isothermal decomposition.

The intermediate was formed from the amorphous lower carbonate phase within a limited range of partial pressure of carbon dioxide (P_{CO_2}), temperature (which also includes the rate of heating) and heating time etc. Typical examples are (1) P_{CO_2} = 1.0 kg cm^{-2}, 476°C (isothermal condition) holding for 0—60 min (maximum at ~10 min), (2) P_{CO_2} = 21 kg cm^{-2}, 450—490°C (maximum at 470°C), (non-isothermal condition; heating at ~10°C min^{-1}) [3]. The amount of intermediate and its characteristics probably depend on the heating condition. The CO_2/MgO molar ratio was higher in the intermediate than the lower carbonate as reported in a previous paper [3] although the ratio could not exceed 1.00 since this corresponds to $MgCO_3$.

Formation of the intermediate (Fig. 9D, 0—10 minutes) was believed to be exothermic. However, it was not detected by DTA (Fig. 6C) since the amount of intermediate was very small (powder X-ray diffraction in Figs. 9D and 10) and overshadowed by the simultaneous decomposition of the amorphous lower carbonate (TG in Fig. 9B and DTA in Fig. 9C).

The intermediate was believed to decompose into MgO (amorphous or crystalline) since the disappearance of the intermediate was accompanied by a decrease in the CO_2/MgO molar ratio [3] and a simple reverse reaction from the intermediate into the amorphous lower carbonate was difficult to imagine.

The amorphous lower carbonate may consist of multiple phases; the possibility of an amorphous lower carbonate coexisting with a nonstoichiometric composition and amorphous MgO could not be excluded.

$MgCO_3$ was crystallized from the amorphous phase. The X-ray diffraction intensity of the amorphous halo decreased as the crystallization of $MgCO_3$ proceeded (Figs. 9D and 10). The intermediate disappeared gradually as the $MgCO_3$ appeared. However, whether or not the crystallization of $MgCO_3$ depended directly on the existence of the intermediate could not be determined. The intermediate may affect the crystallization as follows; (1) a small amount of the intermediate might form specific nucleation sites for the $MgCO_3$ crystallization, (2) the formation and decomposition of the intermediate and the subsequent crystallization of $MgCO_3$ might proceed independently on different portions of the specimen, and the former might proceed fortuitously due to the rate of formation and decomposition. Simple phase transition from the intermediate to $MgCO_3$ may occur. However, the source of the strong exothermic phenomenon was not this transition since the X-ray diffraction intensity of $MgCO_3$ and the exothermic heat measured were too

great to be explained by the transition. The rate of crystallization of $MgCO_3$ was reduced at low temperatures (Figs. 11 and 12). When the specimen was heated rapidly, the heat of crystallization raised the actual specimen temperature; the rate of crystallization was highly dependent on the temperature (activation energy: 100—300 kcal $mole^{-1}$). The decarbonation rate of $MgCO_3$ was much smaller than that of the lower carbonate as shown in Fig. 5 and the decomposition of $MgCO_3$ proceeded extremely slowly (TG in Fig. 9B and X-ray diffraction in Figs. 9D and 10).

It was assumed in previous papers [2,3] that the rapid evolution of carbon dioxide was due to the decarbonation caused by the heat of $MgCO_3$ crystallization. This assumption was confirmed. The increase in the specimen temperature up to its decomposition temperature occurred only when the crystallization took place at a high temperature, where the rate of crystallization was rapid enough to prevent the dispersion of the heat of crystallization. A rapid evolution of carbon dioxide took place only when the specimen was heated non-isothermally without being held at a constant temperature (Fig. 11). When the rapid evolution of carbon dioxide took place, the heat of crystallization measured by DTA was smaller than when no simultaneous evolution of carbon dioxide took place (Fig. 13). The difference was due to the heat of decomposition. However, only qualitative discussion was attempted in the present work since large experimental errors were associated with the very rapid and very slow exothermic phenomenon.

Crystallization of MgO was compositionally possible when the dehydration was completed. Further reduction of the CO_2/MgO molar ratio after the decarbonation stage I is more favored than the crystallization of MgO. However, the actual crystallization was observed later; in 0—10 minutes at the isothermal holding temperature of 480°C. No detectable growth was observed in the crystallite size in the MgO crystallized at this temperature; it would require a higher temperature or a longer time.

ACKNOWLEDGEMENTS

The authors thank Mr. K. Matusyama and Mr. K. Kojima of the Tokyo Institute of Technology (Department of Inorganic Materials) for assisting in the construction and the operation of the thermobalance.

REFERENCES

1 Y. Sawada, K. Uematsu, N. Mizutani and M. Kato, J. Inorg. Nucl. Chem., 40 (1978) 979.
2 Y. Sawada, K. Uematsu, N. Mizutani and M. Kato, Thermochim. Acta, 27 (1978) 45.
3 Y. Sawada, J. Yamaguchi, O. Sakurai, K. Uematsu, N. Mizutani and M. Kato, Thermochim. Acta, in press.
4 R.M. Dell and S.W. Weller, Trans. Faraday Soc., 55 (1959) 2203.
5 N. Morandi, Mineral. Petrogr. Acta, 15 (1969) 93.
6 H. Hashimoto, T. Tomizawa and M. Mitomo, Kogyo Kagaku Zasshi, 71 (1968) 480.
7 W. Höland and K. Heide, Thermochim. Acta, 15 (1976) 287.

8 J. Suzuki and M. Ito, J. Jpn. Assoc. Mineral. Petrol. Econom. Geol., 69 (1974) 275.
9 Powder Diffraction File, Joint Committee on Powder Diffraction Standards, Swarthmore, U.S.A., 1977, Inorganic 8-176.
10 Powder Diffraction File, Joint Committee on Powder Diffraction Standards, Swarthmore, U.S.A., 1977, Inorganic 8-479.
11 I. Barin and O. Knacke, Thermochemical Properties of Inorganic Substances, Springer, Heidelberg, 1973, pp. 163, 441, 450.